Drifting potential humps in ionization zones: the "propeller blades" of high power impulse magnetron sputtering

André Anders,[1,a)] Matjaž Panjan,[1,2] Robert Franz,[1,3] Joakim Andersson,[1,4] and Pavel Ni[1]

[1] Lawrence Berkeley National Laboratory, 1 Cyclotron Road, Berkeley, California 94720, USA

[2] Jožef Stefan Institute, Jamova 39, 1000 Ljubljana, Slovenia

[3] Montanuniversität Leoben, Franz-Josef-Strasse 18, 8700 Leoben, Austria

[4] Centre for Quantum Technologies, National University of Singapore, 3 Science Drive 2, 117543 Singapore, Singapore

[a)] Author to whom correspondence should be addressed. Electronic mail: aanders@lbl.gov

Abstract

Ion energy distribution functions measured for high power impulse magnetron sputtering show features such as a broad peak at several 10 eV with an extended tail, as well as asymmetry with respect to $\mathbf{E} \times \mathbf{B}$, where $\mathbf{E}$ and $\mathbf{B}$ are the local electric and magnetic field vectors, respectively. Here it is proposed that those features are due to the formation of a potential hump of several 10 V in each of the traveling ionization zones. Potential hump formation is associated with a negative-positive-negative space charge that naturally forms in ionization zones driven by energetic drifting electrons.

High power impulse magnetron sputtering (HiPIMS) combines magnetron sputtering with pulsed power technology. The objective of applying power in pulses, or bursts of pulses, is the ionization of the sputtered atoms. The magnetron is turned into a plasma source delivering ions of the process gas and the target material. This can have great effects on the substrate-film interface and on the microstructure of the films deposited. HiPIMS can be very beneficial especially when dense, smooth, and/or hard coatings are required by the application.

The ion energy in HiPIMS is long recognized as being significantly higher than the ion and atom energies in conventional sputtering. For example, Hecimovic and Ehiasarian[1] show ion energy distribution functions (IEDFs) for singly charged ions exhibiting a thermal energy peak, a non-thermal energy peak, and a long tail. Gudmundsson *et al.*[2] reviewed the field and highlighted the work by Lundin *et al.*[3] who focused on ion energy measurements made from the side of a magnetron. In their example, Ti^{1+} ions show an energy peak at about 12 eV with a tail up to 80 eV.

The general paradigm in magnetron sputtering is that, apart from a small percentage of reflected particles having high energies corresponding to up to the discharge voltage, the energies of sputtered atoms originate from the sputtering process as described by the Sigmund-Thompson random collision cascade model.[4,5] The distribution function is essentially determined by the surface binding energy ε_{SB} of the target atoms,

$$f_{\text{Thompson}}(\varepsilon) \propto \frac{\varepsilon}{(\varepsilon + \varepsilon_{SB})^3} \, . \tag{1}$$

The distribution (1) has a peak at $\varepsilon_{SB}/2$ and falls with ε^{-2}. However, at high energies, when $\varepsilon \gg \varepsilon_{SB}$, expression (1) is inadequate and a more complete formula needs to be used,[5-7] namely one that accounts for the energy of incident ions, ε_i, and for the mass ratio of incoming ion and target atoms, as follows[5,7]

$$f_{\text{Thompson}}\left(\varepsilon\right) = \begin{cases} A\dfrac{\varepsilon\left[1-\sqrt{\left(\varepsilon_{SB}+\varepsilon\right)/\Lambda\,\varepsilon_i}\,\right]}{\left(\varepsilon+\varepsilon_{SB}\right)^3} & if\ 0 \le \varepsilon \le \Lambda\,\varepsilon_i \\[4mm] 0 \quad if\ \varepsilon > \Lambda\,\varepsilon_i \end{cases} \tag{2}$$

where

$$\Lambda = \frac{4m_i m_t}{\left(m_i+m_t\right)^2} \tag{3}$$

and A is a normalization factor. For self-sputtering, the masses of ions m_i and target atoms m_t are equal, and hence $\Lambda = 1$. For very different masses, Λ can be much smaller than unity, and the distribution function is reduced at high energies (Fig. 1).

The energy of ions of the target material is originally determined by the energy distribution of sputtered atoms, Eq. (2), but may be greatly modified as soon as the ionization process occurs since ions are subject to electric fields that may be present. It is generally accepted that ions are accelerated back to the target as soon as ionization occurs, provided ionization occurred near the target, where the gradient of the plasma potential points to the target.[8,9] Atoms ionized further away from the target have a greater chance to escape and to reach the substrate where they contribute to film growth. Ions may be scattered by the background gas and thermalized by collisions, i.e. the IEDF exhibits a reduced tail especially at high pressure. Should ions arrive in the near-substrate region they are subject to acceleration in the sheath next to the substrate, gaining energy proportional to the substrate sheath voltage and ion charge state number. We will show that this paradigm is incomplete and that localized, drifting potential humps and associated electric fields can explain certain features of the IEDF and other properties.

Experimentally determined IEDFs show features such as additional broad peaks[1] and azimuthal asymmetry[3,10] (we consider here magnetrons with round targets, for simplicity, where the term "azimuthal" can be applied). As an example, Fig. 2 shows the energy distribution functions as measured from the side of a planar 76 mm (3 inch) magnetron (details are provided in ref.[11]). One can see that the doubly charged ions have approximately twice the energy of singly charged ions, suggesting acceleration in an electric field. The dependence of the measured energy distribution on direction, $\mathbf{E} \times \mathbf{B}$ versus $-\mathbf{E} \times \mathbf{B}$, shows that acceleration must occur near the magnetron where the $\mathbf{E} \times \mathbf{B}$ condition applies, as opposed to acceleration in the sheath of the measuring instrument.

Ion acceleration *away* from the target region is peculiar because positive ions are generally attracted *towards* the target, which is the cathode of the discharge. Measurements of the plasma potential *averaged over many pulses* showed that the average field

$$\mathbf{E} = -\nabla V_{pl} \tag{4}$$

is indeed directed towards the target,[8,9,12] which is expected and necessary to obtain the desired sputtering effects. We stress that the measurements[8,9,12] were done with averaging over 100 or more pulses, therefore information associated with localized, drifting zones was lost. The existence of such drifting ionization zones (a.k.a. plasma inhomogeneities, bunches, spokes) was independently reported by several groups.[13-15] An example of a fast camera image is shown in Fig. 3(a). Short-exposure and streak side-on images of such zones indicate localized disruption of the closed electron drift, and the formation of plasma flares.[16] It was suggested[16-18] that the electric field over the racetrack has a parallel component E_ξ which is responsible for disruption of electron trapping and formation of plasma flares (ξ is the coordinate tangential to the racetrack in a plane parallel to the target surface).

It is well-established in plasma physics that a potential difference and its related electric field can be associated with a space-charge double layer.[18-20] In general, the Poisson equation

$$\nabla \mathbf{E} = \rho / \varepsilon_0 , \tag{5}$$

associates the gradient of the electric field with the space charge $\rho = e\left(\overline{Q} n_i - n_e\right)$, where ε_0 is the permittivity, e is the elementary charge, $\overline{Q}$ is the mean ion charge state, n_i and n_e are the densities of ions and electrons, respectively. Using (4) gives the Poisson equation in the form $\nabla^2 V = -\rho / \varepsilon_0$, explicitly connecting space charge and potential. With these expressions, different space charge assumptions and their consequences for field and potential can be discussed.

Fig. 3(b) illustrates the general fact that the potential on the sides of a double layer is different (*cf.* Brenning *et al.*,[18] and Piel *et al.*[20]) However, for a closed racetrack, the potential needs to be reproduced when returning to the same location. For round targets, where ξ could be the azimuthal angle, this requirement can be expressed as

$$\int_0^{2\pi} \frac{\partial V(\xi)}{\partial \xi} d\xi = 0 . \tag{6}$$

Since there may be more than one ionization zone over the racetrack, the relation

$$\int_{\xi_{start}}^{\xi_{end}} \frac{\partial V(\xi)}{\partial \xi} d\xi \approx 0 \tag{7}$$

4

should hold, leading to $V\left(\xi_{start}\right) \approx V\left(\xi_{end}\right)$, where ξ_{start} and ξ_{end} refer to the beginning and end coordinates of one ionization zone in the ξ-direction. In other words, while a local field should exist to explain phenomena such as flare formation,[16,21] the total potential drop along an ionization zone is approximately zero. This implies the existence of *two* double layers, one at each boundary, with opposite order of space charge such that the voltage drops cancel. A close proximity of ionization zone boundaries leads to a potential maximum, i.e. a potential hump (Fig. 3(c)). The observation of narrow, somewhat triangularly shaped ionization zones, as shown in Fig. 3(a), suggests that the layer system may be asymmetric, as shown in Fig. 3 (d).

One consequence of the electric field structure is that the local $\mathbf{E} \times \mathbf{B}$ produces electron drift away from the target for $E_{\xi} > 0$, leading to the already-reported plasma flares.[16] However, somewhat surprisingly, the region were $E_{\xi} < 0$ must cause drift of electrons towards the target, where electrons are expected to be reflected by the sheath. Most likely, this situation promotes turbulence, which we see in (unpublished) probe data and fast camera images.

A potential hump in the center of each ionization zone is in agreement with experimentally observed features of ion energy, like those shown in Fig. 2. Ions formed at high potential in the ionization zone are accelerated away from the zone in *all* directions, including toward the substrate and radial directions.

Since the ionization zones travel in the $\mathbf{E} \times \mathbf{B}$ direction, ions moving in the direction parallel to $\mathbf{E} \times \mathbf{B}$ are surfing on the potential gradient longer than ions moving antiparallel to $\mathbf{E} \times \mathbf{B}$, thereby producing the azimuthal asymmetry seen in Fig. 2. As seen in the laboratory frame of reference, where the measuring instrument is anchored, ions surfing the potential hump in the $\mathbf{E} \times \mathbf{B}$ direction gain energy from the potential and kinetic energies of the hump, hence their energy is

$$E_i = E_0 + \frac{m_i}{2} v_{IZ}^2 + eQV_{hump} \tag{8}$$

where E_0 represents the energy from the sputtering and collisional processes, v_{IZ} is the drift velocity of the ionization zone, Q is the ion charge state number, and V_{hump} is the height of the potential hump. Ions moving in the opposite direction also gain the potential energy but their velocity is reduced by the effect of the hump drift:

$$E_i = E_0 - \frac{m_i}{2} v_{IZ}^2 + eQV_{hump} \tag{9}$$

Expressing the drift effect by an equivalent kinetic energy change $eV_{drift} = \pm m v_{IZ}^2 / 2$, and using the example data shown in Figure 2, we obtain approximately $V_{hump} \approx 35 \, \text{V}$ and

$V_{drift} \approx 25$ V. The latter value can be cross-checked using the drift speed measurement of the ionization zone, $v_{IZ} = 7000$ m/s for Nb in Ar,[14] and obtain $V_{drift} \approx 24$ V, which is in rather good agreement. Broad features of IEDFs suggest that potential humps are in the range of 10-50 V, which is compatible with time-resolved measurements of variations of floating and plasma potentials[14,15] (though it is difficult to directly measure the plasma potential in the interesting locations since probes greatly disturb the discharge). One can conclude that, figuratively speaking, the traveling potential humps of ionization zones resemble the blades of a propeller giving particles energy and a preferred flow direction.

The question remains what mechanism would lead to space charge distributions as shown in Figs. 3(c) or (d). Double layers form when charges are separated or trapped by some means. In our case, consistent with an earlier interpretation of ionization zone motion,[17] trapping is related to electron impact ionization and ion inertia, as follows. Electrons drifting in the $\mathbf{E} \times \mathbf{B}$ direction experience a greater likelihood of interaction when encountering a region of enhanced particle density; electron slowing may lead to a thin negative space charge layer at the trailing edge of the ionization zone (left edge in Fig. 3(a)). A dense plasma zone is formed at the locations of greatest electron-ion and electron-neutral interaction. Electrons drift from this zone with a velocity of about $\mathbf{E} \times \mathbf{B}/B^2$ along the racetrack and in the z-direction, depending on the local field direction. Electrons leave ions behind, temporarily forming a positive space charge. Formation of the positive space charge is a transient effect due to ion inertia with a characteristic time of the inverse ion plasma frequency.[22] The electrons from the ionization zone spread in the $\mathbf{E} \times \mathbf{B}$ direction and produce there a slight negative space charge. Therefore, the negative-positive-negative space charge structure can be readily associated with the peculiarities of an ionization zone under the magnetron's $\mathbf{E} \times \mathbf{B}$ condition. The motion of the ionization zone is primarily determined by "evacuating" ions from the location of ionization, causing electrons to drift a bit further, through the evacuated region, before encountering a region of enhanced particle density.[17] Therefore, conditions leading to the potential hump and drift of the ionization zone are related. Suitable simulations of these processes are needed to underpin the proposed mechanism in a quantitative way. Important steps have already been taken for example by Gallian *et al.*[23] who essentially found that density variations along the racetrack can be described by a system of advection, diffusion and reaction equations. To make the situation manageable, a number of simplifying assumptions had to be made, among them that quasi-neutral conditions apply everywhere, therefore, the here-proposed potential hump mechanism could not be produced. Future work will require replacing the quasineutrality assumption with a solution of the Poisson equation.

In summary, we propose that ionization zones in high power impulse magnetron sputtering are locations of locally enhanced potential. Such potential structures can explain the disruption of closed electron drift, formation of plasma flares, relatively high energy of ions at

the substrate, and the difference of ion energy distribution functions with respect to the $\mathbf{E} \times \mathbf{B}$ drift direction.

References

[1] A. Hecimovic and A. P. Ehiasarian, J. Appl. Phys. **108,** 063301 (2010).

[2] J. T. Gudmundsson, N. Brenning, D. Lundin, and U. Helmersson, J. Vac. Sci. Technol. A **30,** 030801 (2012).

[3] D. Lundin, P. Larsson, E. Wallin, M. Lattemann, N. Brenning, and U. Helmersson, Plasma Sources Sci. Technol. **17,** 035021 (2008).

[4] P. Sigmund, Phys. Rev. **184,** 383 (1969).

[5] M. W. Thompson, Phil. Mag. **18,** 377 (1968).

[6] J. Vlček, P. Kudláček, K. Burcalová, and J. Musil, Eur. Phys. Lett. **77,** 45002 (2007).

[7] V. V. Serikov and K. Nanbu, J. Appl. Phys. **82,** 5948 (1997).

[8] J. W. Bradley, S. Thompson, and Y. A. Gonzalvo, Plasma Sources Sci. Technol. **10,** 490 (2001).

[9] A. Rauch, R. Mendelsberg, J. M. Sanders, and A. Anders, J. Appl. Phys. **111,** 083302 (2012).

[10] P. Poolcharuansin, B. Liebig, and J. W. Bradley, Plasma Sources Sci. Technol. **21,** 015001 (2012).

[11] M. Panjan, R. Franz, and A. Anders, Plasma Sources Sci. Technol.**,** in preparation (2013).

[12] A. Mishra, P. J. Kelly, and J. W. Bradley, J. Phys. D: Appl. Phys. **44,** 425201 (2011).

[13] A. Kozyrev, N. Sochugov, K. Oskomov, A. Zakharov, and A. Odivanova, Plasma Physics Reports **37,** 621 (2011).

[14] A. Anders, P. Ni, and A. Rauch, J. Appl. Phys. **111,** 053304 (2012).

[15] A. P. Ehiasarian, A. Hecimovic, T. de los Arcos, R. New, V. Schulz-von der Gathen, M. Böke, and J. Winter, Appl. Phys. Lett. **100,** 114101 (2012).

[16] P. A. Ni, C. Hornschuch, M. Panjan, and A. Anders, Appl. Phys. Lett. **101,** 224102 (2012).

[17] A. Anders, Appl. Phys. Lett. **100,** 224104 (2012).

[18] N. Brenning, D. Lundin, T. Minea, C. Costin, and C. Vitelaru, J. Phys. D: Appl. Phys. **46,** 084005 (2013).

[19] C. Charles, Plasma Sources Sci. Technol. **16,** R1 (2007).

[20] A. Piel, E. Möbius, and G. Himmel, Astrophysics and Space Science **72,** 211 (1980).

[21] J. Andersson, P. Ni, and A. Anders, Appl. Phys. Lett. **103,** 054104 (2013).

[22] A. Anders, Surf. Coat. Technol. **183,** 301 (2004).

[23] S. Gallian, W. N. G. Hitchon, D. Eremin, T. Mussenbrock, and R. P. Brinkmann, Plasma Sources Sci. Technol. **22,** 055012 (2013).

Figure Captions

Fig. 1 Energy distribution of sputtered atoms based on the collision cascade theory, for an assumed surface binding energy of 5 eV, showing the simplified Sigmund-Thompson approximation, Eq. (1), and the full formula, Eq. (2), for incident ions with energies of 500 eV and 1000 eV, as indicated. The mass parameter Λ is unity for self-sputtering and smaller for very mismatched ion-atom masses, using here the example of La and B, as applicable to HiPIMS of LaB_6.

Fig. 2 Ion energy distribution function measured with a Hiden EQP300 energy analyzer in 140 mm distance from the target, recording niobium ions emitted near the target plane tangentially from the racetrack; discharge voltage 350 V, 200 μs pulse length, 100 pulses per second, 275 A peak, in 0.53 Pa of Ar.

Fig. 3 Ionization zones and potential distribution: (a) image of an ionization zone, Nb target, taken with 100 ns exposure time; arrows indicate drift direction, for details see[14]; (b) space charge ρ, electric field $\mathbf{E}$ and potential V similar to model assumptions of ref.[18]; (c) a symmetric pair of double layers resulting in a potential hump, with equal potential on each side of the ionization zone; (d) an asymmetric pair of double layers, also resulting in a potential hump but addressing the asymmetric shape of the ionization zone.
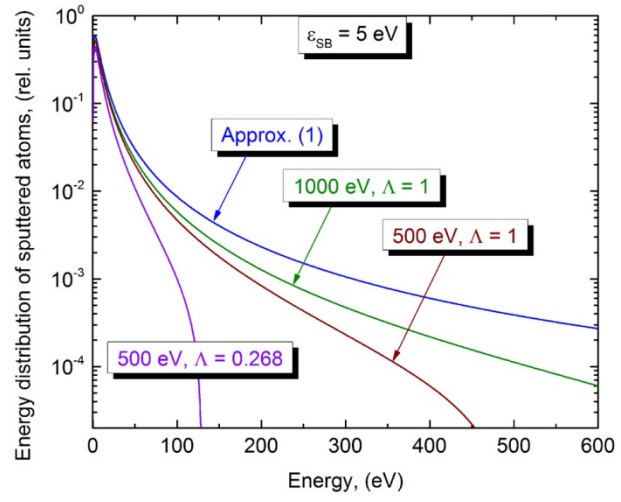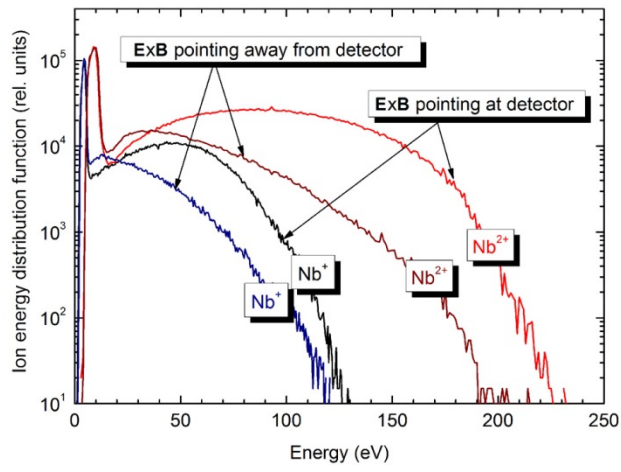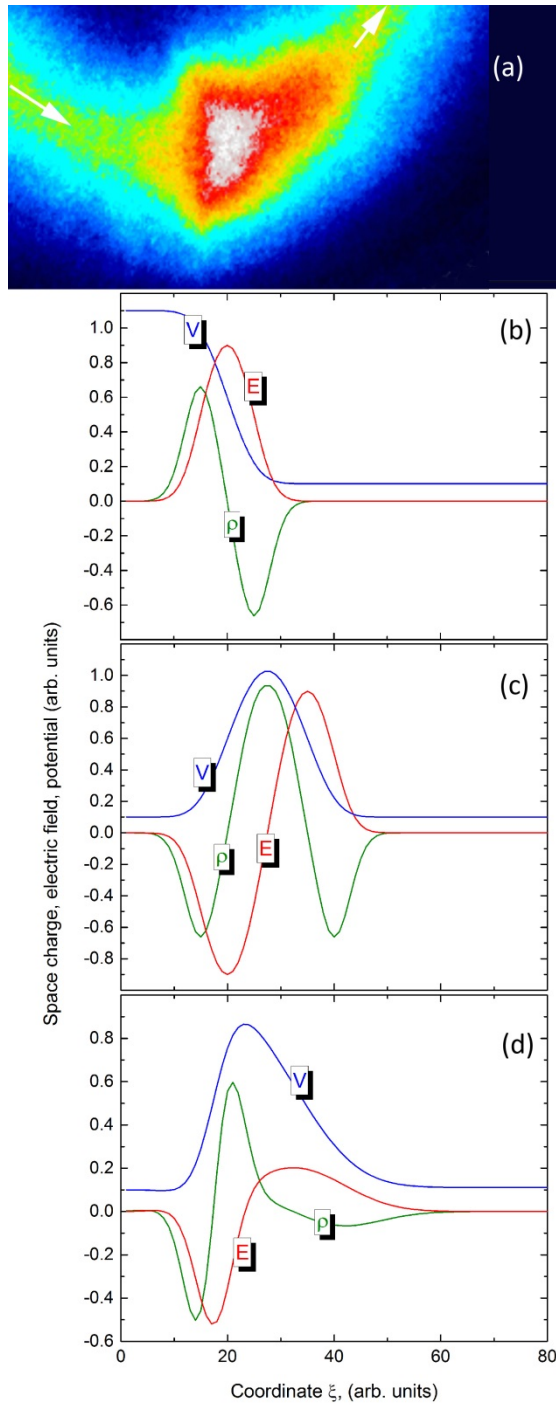
Fig. 1

Fig. 2

Fig. 3